An Arbitrary Higher-Order Discontinuous Galerkin-Spectral Deferred Correction Scheme for the Variable Coefficients Advection Equation

Jing Wang, Chunya Wu, Lingzhi Qian*

***Abstract*—In this paper, a discontinuous Galerkin-spectral deferred correction (DG-SDC) scheme for the advection equation with variable coefficients is presented. In spatial discretization, we consider the discontinuous Galerkin (DG) method to discrete the variable coefficients advection equation. In time discretization, we introduce the spectral deferred correction (SDC) method to obtain the full-discrete scheme. The proposed scheme can reach arbitrary higher-order accuracy in space and time. However, in the process of numerical calculation, the advection equation produces numerical oscillations near the strong discontinuities. To prevent the onset of spurious oscillations, we introduce two kinds of vertex-based slope limiters to modify the full-discrete scheme. Therefore, we can get a more stable and efficient numerical scheme. Finally, some numerical tests are illustrated to confirm the validity and higher-order accuracy of the proposed scheme.**

***Index Terms*—Discontinuous Galerkin method, Spectral deferred correction method, Slope limiter, Variable coefficients advection equation, Higher-order scheme.**

I. Introduction

The DG method is one of the most popular numerical methods, especially for Hyperbolic conservation law. This method was first proposed by Reed and Hill for solving hyperbolic equations in [21]. DG method has lots of advantages, such as high parallelizability, localizability and easy handing of complicated geometries. Therefore, DG method has been widely used in solving various types of PDEs (see, e.g., [2], [8], [16], [17], [19]). However, the solutions of the advection equation might contain strong discontinuities on boundary layers. The DG method can capture weak discontinuities without further modification. But for problems with strong shocks or contact discontinuities, the numerical solution might have significant spurious oscillations near the strong shocks or contact discontinuities [28]. Thus, to prevent the onset of spurious oscillations, various limiters have been introduced into numerical calculation. For example, Tran proposed a slope-reconstruction methodology to perform second-order enhancement by using slope-limiters for the simultaneous linear advection of several scalar variables in [25]. Zhu and Shu proposed the Runge-Kutta DG scheme with multi-resolution weighted essentially non-oscillatory (WENO) limiters, this scheme was applied to solve steady Euler equations in [29]. In order to solve compressible Euler equations in two dimensions, Yu et al. proposed the Hermite-WENO DG method to obtain a higher-order accuracy scheme in [19]. In this paper, we introduce two types of limiter to suppress spurious oscillation in spatial discretization. The slope limiter mainly passes through restricting some of the degrees of freedom to certain bounds so that eliminates over- and undershoots. All slope limiters attempt to modify the discrete solution in a suitable way while preserving higher-order accuracy as much as possible. Based on this idea, various slope limiters have been applied to various numerical solutions (see, e.g., [7], [20], [23], [16]).

The SDC method was developed by Dutt in [6] to solve the cauchy problem for ordinary differential evolution problem. Then it is extended by Kress and Gustafsson to the initial boundary value problems in [12]. In recent years, the SDC method has been applied to solve the various partial differential equations (PDEs) to obtain the higher order time scheme for these system of PDEs. For example, Weng et al. used operator splitting method and SDC method to solve the molecular beam epitaxy equation in [27]. Guo and Xu proposed invariant energy quadratization approach and SDC method to solve Phase field problems, and obtained a decoupled, unconditionally energy stable and higher-order accuracy scheme in [9]. To capture the complex processes involved in atmospheric flows over long periods of time, Hamon et al. proposed implicit-explicit splitting method and SDC method to solve shallow water equations in [10]. Similarly, we introduce the SDC method to obtain a time discrete scheme with arbitrary higher-order accuracy in this paper. The basic ideal of SDC method is to reduce the error of the low-order time stepping scheme by iteratively solving the Picard integral equation in an iterative framework to achieve any convergence order (see, e.g., [5], [6], [14], [4], [24]). In this procedure, the lower-order scheme sweeps repeatedly through subintervals to update the provisional solution. Finally, the time discrete scheme can achieve the desired accuracy.

In this paper, we propose a numerical scheme that combines the advantages of DG and SDC methods for the variable coefficients advection equation, which can simultaneously achieve arbitrary higher-order accuracy in space and time. Meanwhile, to prevent the onset of spurious oscillations

Manuscript received May 6, 2022; revised October 17, 2022. This work was supported in part by the the NSF of China (No. 11861054), Natural Science Foundation of Guangxi (No. 2020GXNSFAA297223), Innovation Project of Guangxi Guaduate Education(No. JGY2021028), English curriculum construction project of Guangxi Normal University (No. 2021XJQYW04) and Innovation Project of Guangxi Graduate Education (No. YCSW2022185).

Jing Wang is a graduate student of the College of Mathematics and Statistics in Guangxi Normal University, Guilin 541006, P.R. China (e-mail:jingwang@stu.gxnu.edu.cn).

Chunya Wu is a graduate student of the College of Mathematics and Statistics in Guangxi Normal University, Guilin 541006, P.R. China (e-mail:chunyawu00@stu.gxnu.edu.cn).

*Lingzhi Qian is an professor of the College of Mathematics and Statistics in Guangxi Normal University, Guilin 541006, P.R. China, Department of Mathematics, College of Sciences, Shihezi University, Shihezi 832003, P.R. China (corresponding author, e-mail: qianlz@mailbox.gxnu.edu.cn).

near the strong discontinuities, we introduce two kinds of slope limiters to obtain a more stable and efficient numerical scheme. The arbitrary higher-order accuracy of the proposed scheme and the performance of slope limiters are verified by numerical examples.

The outline of the paper is organized as follows: We recall the classical advection equation with variable coefficients and introduce the spatial semi-discrete scheme in Section 2. In Section 3, the full-discrete numerical scheme is presented based on the SDC method. In addition, we introduce the detailed slope limiting algorithms to obtain a modified full-discrete scheme which can prevent the onset of spurious oscillations near the strong discontinuities in Section 4. Various numerical tests are given to validate the higher-order accuracy, efficiency and stability of the proposed numerical schemes in Section 5. Some conclusions and future research are drawn in Section 6.

II. Spatial semi-discrete scheme

Let $J := [0, t_{\text{End}}]$ be a finite time interval and $\Omega \subset \mathbb{R}^2$ be a polygonally bounded domain with boundary $\partial\Omega$. The initial and boundary value problem of advection with variable coefficients is defined as follows:

$$\begin{cases} \partial_t c(t,\boldsymbol{x}) + \nabla\cdot(\boldsymbol{u}(t,\boldsymbol{x})c(t,\boldsymbol{x})) = f(t,\boldsymbol{x}) \text{ in } J\times\Omega, \\ c = c_D \text{ on } J\times\partial\Omega_{\text{in}}(t), \\ c = c^0 \text{ on } \{0\}\times\Omega, \end{cases} \tag{1}$$

where the unknown $c(t,\boldsymbol{x})$ denotes the solute concentration, $\boldsymbol{u}(t,\boldsymbol{x})$ represents the velocity of fluid which is variable, and $f(t,\boldsymbol{x})$ accounts for generation or degradation of $c(t,\boldsymbol{x})$. The inflow boundary is denoted by $\partial\Omega_{\text{in}}(t) = \{\boldsymbol{x}\in\partial\Omega \mid \boldsymbol{u}(t,\boldsymbol{x})\cdot\boldsymbol{v}(\boldsymbol{x}) < 0\}$, $\boldsymbol{v}(\boldsymbol{x})$ is the outward unit normal. The outflow boundary is represented by $\partial\Omega_{\text{out}} = \partial\Omega/\partial\Omega_{\text{in}}(t)$. The c^0 and c_D are initial and Dirichlet boundary data, respectively.

The classical DG method is introduced to discretize the advection equation with variable coefficients in spatial. It's worth noting that the velocity of fluid $\boldsymbol{u}(t,\boldsymbol{x})$ does not use discrete representation in the boundary integral, because the L^2-projection on elements may have poor approximation quality on edges and generally produce different values on both sides of the edges [22].

Let $\mathcal{T}_h = \{T\}$ denote a regular family of non-overlapping partitions of Ω into K closed triangles T of characteristic size h such that $\overline{\Omega} = \cup T$. For $T\in\mathcal{T}_h$, $\boldsymbol{v}_T$ is the unit normal on ∂T exterior to T. Let Γ_{int} denote the set of interior edges, Γ_{out} is the set of boundary edges, and $\partial\mathcal{T}_h := \Gamma_{int}\cup\Gamma_{out} = \{E\}$ is the set of all edges. For an interior edge $E\in\Gamma_{int}$ shared by triangles T^- and T^+, the one-side values of a scalar $w = w(\boldsymbol{x})$ on E is defined by

$$w^-(\boldsymbol{x}) = \lim_{\varepsilon\to 0^+} w(\boldsymbol{x} - \varepsilon\boldsymbol{v}_{T^-})$$

and

$$w^+(\boldsymbol{x}) = \lim_{\varepsilon\to 0^+} w(\boldsymbol{x} - \varepsilon\boldsymbol{v}_{T^+}), \text{ for } \forall\varepsilon > 0.$$

But for the boundary edge $E\in\Gamma_{out}$, only the definition on the left is meaningful. Finally, the definition of the inner product is introduced as follows:

$$(w,v)_T = \int_{\partial T} wv\, d\boldsymbol{x} \text{ and } \langle\zeta,\rho\rangle_E = \int_E \zeta\rho\, d\boldsymbol{s}. \tag{2}$$

To get variational formulation, we multiply (1) by a smooth test function w and integrate by parts over element $T\in\mathcal{T}_h$. The variational formulation is given by

$$\begin{aligned} &\Big(w, \partial_t c(t,\boldsymbol{x})\Big)_T - \Big(\nabla w\cdot\boldsymbol{u}(t,\boldsymbol{x}), c(t,\boldsymbol{x})\Big)_T \\ &+ \Big\langle w(\boldsymbol{u}(t,\boldsymbol{x})\cdot\boldsymbol{v}_T), c(t,\boldsymbol{x})\Big\rangle_{\partial T} = \Big(w, f(t)\Big)_T. \end{aligned} \tag{3}$$

We denote $\mathcal{P}_p(T)$ by the space of polynomials of degree at most p on $T\in\mathcal{T}_h$. Let $\mathcal{P}_p(T) := \{w_h : \overline{\Omega}\to\mathbb{R}; \forall T\in\mathcal{P}_p(T)\}$ denote the broken polynomial space on the triangulation T. For the spatial semi-discrete scheme, we assume that the coefficient functions are approximated by $\boldsymbol{u}_h \in [\mathcal{P}_p(\mathcal{T}_h)]^2$ and $f_h(t), c_h^0 \in \mathcal{P}_p(\mathcal{T}_h)$. Incorporating the boundary condition in (1), the semi-discrete formulation is given as follows:

For $t\in J$, $\forall T_k\in\mathcal{T}_h$ and $\forall w_h\in\mathcal{P}_p(\mathcal{T}_h)$, we can find $c_h(t)\in\mathcal{P}_p(\mathcal{T}_h)$ which holds

$$\begin{aligned} &\Big(w_h, \partial_t c_h(t,\boldsymbol{x})\Big)_{T_k} - \Big(\nabla w_h\cdot\boldsymbol{u}_h(t,\boldsymbol{x}), c_h(t,\boldsymbol{x})\Big)_{T_k} \\ &+ \Big\langle w_h^-\,(\boldsymbol{u}_h(t,\boldsymbol{x})\cdot\boldsymbol{v}_{T_k}), \hat{c}_h(t,\boldsymbol{x})\Big\rangle_{\partial T_k} = \Big(w_h, f_h(t)\Big)_{T_k}, \end{aligned} \tag{4}$$

where the boundary integral is calculated by the following upwind-side value,

$$\hat{c}_h(t)\Big|_{\partial T_k} = \begin{cases} c_h^-(t,\boldsymbol{x}), \text{ if } \boldsymbol{u}(t,\boldsymbol{x})\cdot\boldsymbol{v}_{T_k}\geq 0 \text{ (outflow from } T_k) \\ c_h^+(t,\boldsymbol{x}), \text{ if } \begin{array}{c}\boldsymbol{u}(t,\boldsymbol{x})\cdot\boldsymbol{v}_{T_k} < 0 \\ \wedge\,\boldsymbol{x}\notin\partial\Omega_{\text{in}} \text{ (inflow into } T_k)\end{array} \\ c_D^+(t,\boldsymbol{x}), \text{ if } \boldsymbol{x}\in\partial\Omega_{\text{in}} \text{ (inflow into } T_k \text{ over)} \end{cases}$$

Then, we denote a finite element basis function $\varphi_{ki} : \overline{\Omega}\to\mathbb{R}$, which is only supported on the triangle $T_k\in\mathcal{T}_h$ and defined arbitrarily. The finite element space $\mathcal{P}_p(T_k)$ is denoted by

$$\mathcal{P}_p(T_k) = span\{\varphi_{ki}\}_{i\in\{1,\cdots,N\}}, \text{ for } \forall k\in\{1,\cdots,K\}, \tag{5}$$

where N is the number of local degrees of freedom.

Thus, the local concentration c_h and local velocity $\boldsymbol{u}_h$ can be represented in terms of the local basis $\{\varphi_{ki}\}_{i\in\{1,\cdots,N\}}$:

$$\begin{aligned} c_h(t,\boldsymbol{x})\Big|_{T_k} &= \sum_{j=1}^{N} C_{kj}(t)\varphi_{kj}(\boldsymbol{x}), \\ \boldsymbol{u}_h(t,\boldsymbol{x})\Big|_{T_k} &= \sum_{j=1}^{N}\sum_{m=1}^{2} U_{kj}^m(t)\boldsymbol{e}_m\varphi_{kj}(\boldsymbol{x}), \end{aligned}$$

where $\boldsymbol{e}_m$ denotes the m-th unit vector in $\mathbb{R}^2$. We assume that there is a uniform polynomial degree p for every element T_k.

Therefore, the semi-discrete formulation (4) with $w_h = \varphi_{ki}$ for $i\in\{1,\cdots,N\}$ yields a time-dependent system whose contribution from T_k reads

$$\begin{aligned} &\sum_{j=1}^{N}\partial_t C_{kj}(t)\Big(\varphi_{ki},\varphi_{kj}\Big)_{T_k} - \sum_{j=1}^{N} C_{kj}(t)\sum_{l=1}^{N}\sum_{m=1}^{2} U_{kl}^m(t)\Big(\partial_{x^m}\varphi_{ki}\varphi_{kl},\varphi_{kj}\Big)_{T_k} \\ &+ \Big\langle\varphi_{k^-i}(\boldsymbol{u}(t)\cdot\boldsymbol{v}_{k^-}), \widehat{C}_h(t)\Big\rangle_{\partial T_k} = \sum_{j=1}^{N} F_{kl}(t)\Big(\varphi_{ki},\varphi_{kl}\Big)_{T_k}, \end{aligned} \tag{6}$$

where the numerical flux $\widehat{C}_h(t)$ is defined as follows

$$\widehat{C}_h(t)\Big|_{\partial T_k} = \begin{cases} \sum_{j=1}^{n} C_{k^-j}(t)\varphi_{k^-j}, \text{ if } \boldsymbol{u}(t,\boldsymbol{x})\cdot\boldsymbol{v}_{T_k} \geq 0 \\ \sum_{j=1}^{n} C_{k^+j}(t)\varphi_{k^+j}, \text{ if } \begin{array}{c}\boldsymbol{u}(t,\boldsymbol{x})\cdot\boldsymbol{v}_{T_k} < 0 \\ \wedge\, \boldsymbol{x} \notin \Gamma_{int}\end{array} \\ c_D^+(t,\boldsymbol{x}), \text{ if } \boldsymbol{x} \in \Gamma_{int} \end{cases} \quad (7)$$

The system (6) can be written in matrix form as

$$M\partial_t C + \left(-G^1 - G^2 + R\right)C = L - K_D, \quad (8)$$

with the representation vector

$$C(t) = [C_{11}(t)\cdots C_{1N}(t)\cdots C_{k1}(t)\cdots C_{KN}(t)]^T .$$

The block matrices and the right-hand side vectors of equation (8) are described as follows:

The mass matrix M is made of K local matrix M_{T_k}, i.e., $M = \text{diag}\left(M_{T_1},\cdots,M_{T_K}\right)$ with

$$M_{T_k} = \begin{bmatrix} (\varphi_{k1},\varphi_{k1})_{T_k} & \cdots & (\varphi_{k1},\varphi_{kN})_{T_k} \\ \cdots & \cdots & \cdots \\ (\varphi_{kN},\varphi_{k1})_{T_k} & \cdots & (\varphi_{kN},\varphi_{kN})_{T_k} \end{bmatrix}.$$

Similar to the structure of matrix M, the matrices $G^m = \text{diag}(G^m_{T_1},\cdots,G^m_{T_K})$ $(m \in \{1,2\})$ are block matrix with local matrices

$$G^m_{T_k} = \sum_{l=1}^{N} U^m_{kl}(t) \begin{bmatrix} (\partial_{x^m}\varphi_{k1}\varphi_{kl},\varphi_{k1})_{T_k} & \cdots & (\partial_{x^m}\varphi_{k1}\varphi_{k1},\varphi_{kN})_{T_k} \\ \cdots & \cdots & \cdots \\ (\partial_{x^m}\varphi_{kN}\varphi_{k1},\varphi_{k1})_{T_k} & \cdots & (\partial_{x^m}\varphi_{kN}\varphi_{k1},\varphi_{kN})_{T_k} \end{bmatrix}.$$

The vector $L(t)$ is obtained by M times the representation vector of $f_h(t)$, i.e.,

$$L(t) = M\ [F_{11}(t)\cdots F_{1N}(t)\cdots\cdots F_{k1}(t)\cdots F_{KN}(t)]^T.$$

Then, considering the integral over the interior edges Γ_{int} and the boundary edges Γ_{out}, the matrix R is given by $R = R_{int} + R_{out}$. On the interior edges, considering a fixed triangle $T_k = T_{k^-}$ with an interior edge $E_{k^-n^-} \in \partial T_{k^-} \cap \Gamma_{int} = \partial T_{k^-} \cap T_{k^+}$ $(n^- \in \{1,2,3\})$, we obtain entries in the diagonal or off-diagonal blocks of R_{int} from (7). The diagonal blocks of the component-wise are given by

$$[R_{int}]_{(k-1)N+i,(k-1)N+j} = \sum_{E_{kn}\in\partial T_k\cap\Gamma_{int}} \left\langle \varphi_{ki}(\boldsymbol{u}\cdot\boldsymbol{v}_{kn})\delta_{\boldsymbol{u}\cdot\boldsymbol{v}_{kn}\geq 0}, \varphi_{kj}\right\rangle_{E_{kn}},$$

with

$$\delta_{\boldsymbol{u}\cdot\boldsymbol{v}_{kn}\geq 0} := \begin{Bmatrix} 1, \text{ if } u(t,\boldsymbol{x})\cdot\boldsymbol{v}_{T_k} \geq 0 \\ 0, \text{ if } u(t,\boldsymbol{x})\cdot\boldsymbol{v}_{T_k} < 0 \end{Bmatrix}.$$

Entries in off-diagonal blocks of R_{int} are possibly non-zero only for pairs of triangles T_{k^-}, T_{k^+} with $\partial T_{k^-} \cap \partial T_{k^+} \neq \emptyset$, we have

$$[R_{int}]_{(k^--1)N+i,(k^+-1)N+j} = \left\langle \varphi_{k^-i}(\boldsymbol{u}\cdot\boldsymbol{v}_{kn})\delta_{\boldsymbol{u}\cdot\ \boldsymbol{v}_{k^-n^-}<0}, \varphi_{k^+j}\right\rangle_{E_{kn}}$$

with $\delta_{\boldsymbol{u}\cdot\ \boldsymbol{v}_{k^-n^-}<0} := 1 - \delta_{\boldsymbol{u}\cdot\ \boldsymbol{v}_{k^-n^-}\geq 0}$.

Similarly, the consist of entries in the block diagonal matrix R_{out} is given as follows

$$[R_{out}]_{(k-1)N+i,(k-1)N+j} = \sum_{E_{kn}\in\partial T_k\cap\Gamma_{out}} \left\langle \varphi_{ki}(\boldsymbol{u}\cdot\boldsymbol{v}_{kn})\delta_{\boldsymbol{u}\cdot\ \boldsymbol{v}_{kn}\geq 0}, \varphi_{kj}\right\rangle_{E_{kn}},$$

and the right-hand side vector K_D is denoted by

$$[K_D]_{(k-1)N+i} = \sum_{E_{kn}\in\partial T_k\cap\Gamma_{int}} \left\langle \varphi_{ki}(\boldsymbol{u}\cdot\boldsymbol{v}_{kn})\delta_{\boldsymbol{u}\cdot\ \boldsymbol{v}_{kn}\geq 0}, c_D(t)\right\rangle_{E_{kn}}.$$

III. Full-discrete scheme

The spatial semi-discrete system (8) is equivalent to

$$M\partial_t C = V(t) - A(t)C(t) := S\left(C(t),t\right), \quad (9)$$

where $A(t) = -G^1(t) - G^2(t) + R(t)$ and right-hand side vector $V(t) = L(t) - K_D(t)$. We discretize system (9) in time by using the SDC method, which can obtain an arbitrary higher-order accuracy time discrete scheme [3].

Let $0 = t^1 < t^2 < \cdots < t_{\text{End}}$ be a not necessary equidistant decomposition of the time interval J and $\Delta t^n = t^{n+1} - t^n$ denote the length of the interval $[t^n, t^{n+1}]$. We subdivide the interval $[t^n, t^{n+1}]$ into M substeps $t^n = t^n_1 < t^n_2 < \cdots < t^n_M = t^{n+1}$, and $\Delta t^n_m = t^n_{m+1} - t^n_m$ $(m \in \{1,\cdots,M\})$ denotes the length of the m-th subinterval. In addition, C^n_m denotes the discrete solution vector in $t = t^n_m$, i.e., $C^n_m = C(t^n_m)$. Let $C^{n,[k]}_m$ represent the provision solution C^n_m updated after k iterations and $IC^{[k]}(t)$ denote the corresponding Lagrange interpolation polynomial which is constructed by $C^{n,[k]}_m$. So the SDC time discrete scheme is given as follows.

In the prediction process, Euler method is used to solve a set of initial provision solutions at each substep. The initial approximation $C^{n,[0]}_m$ is obtained by the following scheme to traverse the interval $[t^n, t^{n+1}]$

$$C^{n,[0]}_m = C^{n,[0]}_{m-1} + H_{m-1}(C^{[0]}),\ m = 1,\cdots,M, \quad (10)$$

where $C^{0,[0]}_0 = C_0$, $C^{0,[k]}_0 = C_0$ and $H_{m-1}(C)$ is an approximation of $\int_{t^n_{m-1}}^{t^n_m} M^{-1}S(C(t),t)\ dt$. Considering the explicit Euler method, the predictor is yielded by

$$C^{n,[0]}_m = C^{n,[0]}_{m-1} + \Delta t^n_m M^{-1}S\left(C^{n,[0]}_{m-1}, t^n_{m-1}\right). \quad (11)$$

In the process of correction, our goal is to reduce the errors of the provisional solutions by a correction equation. In this paper, we introduce the Lagrange interpolation polynomial of provisional solutions to construct correction equation [6], which is defined as

$$\delta^{[k]}(t) = C(t) - IC^{[k]}(t). \quad (12)$$

Further, the residual function is introduced by

$$\varepsilon^{[k]}(t) = C_0 + \int_{t_0}^{t} M^{-1}S(IC^{[k]}(\tau),\tau)\ d\tau - IC^{[k]}(t). \quad (13)$$

Subtracting (12) from (13) and then differentiating it, the error equation is given as follows

$$\partial_t(\delta^{[k]}(t) - \varepsilon^{[k]}(t)) = \partial_t C(t) - M^{-1}S\left(IC^{[k]}(t),t\right). \quad (14)$$

Using equations (9) and (12), the error equation (14) can be rearranged as follows

$$\begin{aligned}\partial_t(\delta^{[k]}(t) - \varepsilon^{[k]}(t)) =& M^{-1}S\left(IC^{[k]}(t),t\right) \\ &+ \delta^k(t) - M^{-1}S\left(IC^{[k]}(t),t\right).\end{aligned} \quad (15)$$

To solve the error equation (15) by a time integration scheme in the subintervals, we obtain the following difference equation by explicit Euler method

$$\begin{aligned}\delta^{n,[k]}_m =& \delta^{n,[k]}_{m-1} + \varepsilon^{[k]}(t^n_m) - \varepsilon^{[k]}(t^n_{m-1}) + H_{m-1}(C^{[k]} + \delta^{[k]}) \\ &- H_{m-1}(C^{[k]}),\ m = 1,\cdots,M,\end{aligned} \quad (16)$$

where $\delta^{n,[k]}_m$ represents the approximation of $\delta^{[k]}(t^n_m)$.

Finally, substituting (12) and (13) to (16) and defining the new approximate solution by $C_m^{n,[k+1]} = C_m^{n,[k]} + \delta_m^{n,[k]}$, we get the following update equation

$$\begin{aligned} C_m^{n,[k+1]} =& C_{m-1}^{n,[k]} + H_{m-1}(C^{[k+1]}) - H_{m-1}(C^{[k]}) \\ &+ \int_{t_{m-1}^n}^{t_m^n} M^{-1} S\left(IC^{[k]}(\tau), \tau\right) d\tau, \end{aligned} \tag{17}$$

the $S(IC^{[k]}(\tau), \tau)$ in equation (17) is usually approximated by its Lagrange interpolation polynomial $IS^{[k]}(\tau)$, i.e.,

$$\int_{t_{m-1}^n}^{t_m^n} M^{-1} S\left(IC^{[k]}(\tau), \tau\right) d\tau \approx \int_{t_{m-1}^n}^{t_m^n} M^{-1} IS^{[k]}(\tau)\ d\tau := S_m^k, \tag{18}$$

Then the integration (18) is approximated by a numerical quadrature formula, i.e.,

$$S_m^k = \Delta t_m^n \sum_{m=0}^{M} w_{n,m}^k M^{-1} IS^{[k]}\left(C(t_m^n), t_m^n\right), \tag{19}$$

where $w_{n,m}^k$ is equivalent to the integral of the k-th Lagrange interpolation polynomial $M^{-1}IS^{[k]}(t)$ over subinterval $[t_{m-1}^n, t_m^n]$ and then normalized it with Δt_m^n.

IV. Modified full-discrete scheme

Based on the obtained full-discrete scheme in Section 3, we restrict some of the degrees of freedom in each element to prevent the onset of spurious oscillations near the strong discontinuities by the slope limiters, which generates a more stable modified full-discrete scheme.

A. Taylor basis representation

Due to most of limiting procedures rely on some fundamental properties of a certain choice of basis. Similar to [13], the Taylor basis is introduced in this paper. Considering the representation of local solutions $c_h \in \mathcal{P}_p(T_k)$ on two-dimensional Taylor basis, we have

$$\begin{aligned} c_h(\boldsymbol{x}) =& \bar{c}_h\phi_{k1} + \left((\frac{\partial c_h}{\partial x^1})(\boldsymbol{x}_{kc})\Delta(x_k^1)\right)\phi_{k2}(\boldsymbol{x}) \\ &+ \left((\frac{\partial c_h}{\partial x^2})(\boldsymbol{x}_{kc})\Delta(x_k^2)\right)\phi_{k3}(\boldsymbol{x}) \\ &+ \sum_{i=4}^{N_p} \left(\partial^{\boldsymbol{a}_i} c_h(\boldsymbol{x}_{kc})(\Delta\boldsymbol{x}_k)^{\boldsymbol{a}_i}\right)\phi_{ki}(\boldsymbol{x}) \text{ on } T_k \in \mathcal{T}_h, \end{aligned} \tag{20}$$

where ϕ_{ki} represents the Taylor basis function, they are defined as follows:

$$\phi_{k1} = 1,\ \phi_{k2} = \frac{x_k^1 - x_{kc}^1}{\Delta(x_k^1)},\ \phi_{k3} = \frac{x_k^2 - x_{kc}^2}{\Delta(x_k^2)},$$
$$\phi_{ki} = \frac{(\boldsymbol{x} - \boldsymbol{x}_{kc})^{\boldsymbol{a}_i} - \overline{(\boldsymbol{x} - \boldsymbol{x}_{kc})^{\boldsymbol{a}_i}}}{\boldsymbol{a}_i!(\Delta\boldsymbol{x}_k)^{\boldsymbol{a}_i}} \quad \text{for } i \geq 4,$$

and $x_{kc} = [x_{kc}^1, x_{kc}^2]^T$ is the centroid of the T_k. The scaling is giving by $\Delta\boldsymbol{x}_k = [\Delta(x_k^1), \Delta(x_k^2)]^T$ with

$$\Delta(x_k^j) = \frac{(x_{k,\max}^j - x_{k,\min}^j)}{2},\ \text{for } j \in \{1, 2\},$$

where $x_{k,\max}^j$ and $x_{k,\min}^j$ are the minimum and maximum values of the corresponding spatial coordinates on T_k, i.e.,

$$x_{k,\max}^j = \max_{i\in\{1,2,3\}} x_{ki}^j \text{ and } x_{k,\min}^j = \min_{i\in\{1,2,3\}} x_{ki}^j.$$

In addition, the multi-indices $\boldsymbol{a}, \boldsymbol{b}$ and $\boldsymbol{x}^{\boldsymbol{a}}$ are defined as follows:

$$\boldsymbol{a} + \boldsymbol{b} = [a^1 \pm b^1, a^2 \pm b^2]^T,\ |\boldsymbol{a}| = a^1 + a^2,\ \boldsymbol{a}! = a^1!a^2!,$$
$$\boldsymbol{x}^{\boldsymbol{a}} = (x^1)^{a^1}(x^2)^{a^2},\ \partial^{\boldsymbol{a}} = \partial^{|\boldsymbol{a}|}/\partial(x^1)^{a^1}\partial(x^2)^{a^2}.$$

We employ the L^2-projection to transform function c_h from the model basis representation into Taylor basis representation, i.e., for $\forall w_h \in \mathcal{P}_p(T_k)$

$$\left(w_h, \sum_{j=1}^{N} C_{kj}(t)\varphi_{kj}\right)_{T_k} = \left(w_h, \sum_{j=1}^{N} C_{kj}^{\text{Taylor}}(t)\phi_{kj}\right)_{T_k}. \tag{21}$$

Choosing $w_h = \varphi_{ki}$ ($i \in \{1, \cdots, N\}$), the transform equation (21) is rewritten as

$$\sum_{j=1}^{N} C_{kj}(t)\left(\varphi_{ki}, \varphi_{kj}\right)_{T_k} = \sum_{j=1}^{N} C_{kj}^{\text{Taylor}}(t)\left(\varphi_{ki}, \phi_{kj}\right)_{T_k}. \tag{22}$$

Then the equation (22) can be written in matrix form as

$$M_{T_k}[C]_{k,:} = M_{T_k}^{\text{Taylor}}[C^{\text{Taylor}}]_{k,:}, \tag{23}$$

where the local basis transformation matrix M_{T_k} is given as follows

$$M_{T_k}^{\text{Taylor}} = \begin{bmatrix} (\varphi_{k1}, \phi_{k1})_{T_k} & \cdots & (\varphi_{k1}, \phi_{kN})_{T_k} \\ \cdots & \cdots & \cdots \\ (\varphi_{kN}, \phi_{k1})_{T_k} & \cdots & (\varphi_{kN}, \phi_{kN})_{T_k} \end{bmatrix}.$$

Using $M^{\text{Taylor}} = \text{diag}(M_{T_1}^{\text{Taylor}}, \cdots, M_{T_K}^{\text{Taylor}})$ and representation vectors C and C^{Taylor}, we obtain the following linear transformation system

$$MC = M^{\text{Taylor}}C^{\text{Taylor}}. \tag{24}$$

B. Linear vertex-based limiter

Linear vertex-based limiter is one of the most effective methods to control the numerical oscillations, which is improved by Kuzmin [12], [13] and Aizinger [11] from Barth-Jespersen limiter [1]. The goal of this limiter is to determine the maximum admissible slope by a linear reconstruction

$$c_h(\boldsymbol{x}) = c_{kc} + \alpha_{ke}\nabla c_h(\boldsymbol{x}_{kc}) \cdot (\boldsymbol{x} - \boldsymbol{x}_{kc}),\ \text{for } 0 \leq \alpha_{ke} \leq 1, \tag{25}$$

where the function value $c_{kc} = c_h(\boldsymbol{x}_{kc})$ in the centroid $\boldsymbol{x}_{kc}$. We choose the correction factor α_{ke} so that above linear reconstruction (25) is bounded in all vertices $\boldsymbol{x}_{ki} \in T_K$ by the minimum and maximum centroid values of all elements containing $\boldsymbol{x}_{ki}$, i.e.,

$$c_{ki}^{\min} \leq c_h(\boldsymbol{x}_{ki}) \leq c_{ki}^{\max},\ \text{for } \forall T_k \in \mathcal{T}_h,\ \forall i \in \{1, 2, 3\}, \tag{26}$$

with $c_{ki}^{\min} = \min_{\{T_l \in \mathcal{T}_h |\ \boldsymbol{x}_{ki} \in T_l\}} c_{lc}$, $c_{ki}^{\max} = \max_{\{T_l \in \mathcal{T}_h |\ \boldsymbol{x}_{ki} \in T_l\}} c_{lc}$.

To ensure the establishment of (26), the correction factor α_{ke} is defined as follows [12], i.e., for $\forall T_k \in \mathcal{T}_h$, we have

$$\alpha_{ke} = \min_{i\in\{1,2,3\}} \left\{ \begin{array}{r} (c_{ki}^{\max} - c_{kc})/(c_{ki} - c_{kc}),\ \text{if} c_{ki} > c_{ki}^{\max} \\ 1,\ \text{if } c_{ki}^{\min} \leq c_{ki} \leq c_{ki}^{\max} \\ (c_{ki}^{\min} - c_{kc})/(c_{ki} - c_{kc}),\ \text{if } c_{ki} < c_{ki}^{\max} \end{array} \right\}, \tag{27}$$

where c_{ki} is determined by the linear reconstruction (25) in $\boldsymbol{x}_{ki}$, i.e., $c_{ki} = c_{kc} + \nabla c_h(\boldsymbol{x}_{kc}) \cdot (\boldsymbol{x}_{ki} - \boldsymbol{x}_{kc})$. Then, the limited counterpart of DG solution is given as follows

$$\begin{aligned} c_h(\boldsymbol{x}) =& \bar{c}_h \phi_{k1} + \alpha_{ke} \Bigg[\left(\frac{\partial c_h}{\partial x^1}(\boldsymbol{x}_{kc}) \Delta(\boldsymbol{x}_k^1) \right) \phi_{k2}(\boldsymbol{x}) \\ &+ \left(\frac{\partial c_h}{\partial x^2}(\boldsymbol{x}_{kc}) \Delta(\boldsymbol{x}_k^2) \right) \phi_{k3}(\boldsymbol{x}) \Bigg]. \end{aligned} \tag{28}$$

C. Hierarchical vertex-based limiter

In order to limit the nonlinear term rather than simply dropping it, we introduce the higher order Hierarchical vertex-based slope limiter from [12], the main idea is to multiply all derivatives of order q by a common correction factor $\alpha_{ke}^{(q)}$.

Let $\mathcal{A}_q = \{a \in N_0^2 \big| |a| = q\}$ be the set of all two-dimensional multi-indices of order q. The correction factor $\alpha_{ke}^{(q)}$ for each order $q \leq p$ is determined by computing formula (27). The linear vertex-based limiter is applied to all linear reconstructions of derivatives of order $q-1$, i.e., for $\forall a \in \mathcal{A}_{q-1}$, we have

$$\begin{aligned} c_{k,a,i} =& c^{\text{Taylor}}_{k,I(a)} \phi_{k1}(\boldsymbol{x}_{ki}) + c^{\text{Taylor}}_{k,I(a+[1,0]^T)} \phi_{k2}(\boldsymbol{x}_{ki}) \\ &+ c^{\text{Taylor}}_{k,I(a+[0,1]^T)} \phi_{k3}(\boldsymbol{x}_{ki}), \text{ on } T_k \in \mathcal{T}_h, \end{aligned} \tag{29}$$

where $I(a) = \frac{|\boldsymbol{a}|(|\boldsymbol{a}|+1)}{2} + a^2 + 1$. Formally, the correction factor $\alpha_{ke}^{(q)}$ is defined as

$$\alpha_{ke}^{(q)} = \min_{a \in \mathcal{A}_{q-1}} \alpha_{ka}^{(q)}, \tag{30}$$

where the factor $\alpha_{ka}^{(q)}$ is given by

$$\alpha_{ka}^{(q)} := \min_{i \in \{1,2,3\}} \begin{cases} (c_{k,a,i}^{\max} - c_{k,a,c})/(c_{k,a,i} - c_{k,a,c}), & \text{if } c_{a,i} > c_{a,i}^{\max} \\ 1, \text{ if } c_{k,a,i}^{\min} \leq c_{k,a,i} \leq c_{k,a,i}^{\max} \\ (c_{k,a,i}^{\min} - c_{k,a,c})/(c_{k,a,i} - c_{k,a,c}), & \text{if } c_{k,a,i} < c_{k,a,i}^{\max} \end{cases}$$

Thus, the limited DG solution becomes

$$\begin{aligned} c_h(\boldsymbol{x}) =& \bar{c}_h \phi_{k1} + \alpha_{ke}^{(1)} \left(\frac{\partial c_h}{\partial x^1}(\boldsymbol{x}_{kc}) \Delta(\boldsymbol{x}_k^1) \right) \phi_{k2}(\boldsymbol{x}) \\ &+ \alpha_{ke}^{(1)} \left(\frac{\partial c_h}{\partial x^2}(\boldsymbol{x}_{kc}) \Delta(\boldsymbol{x}_k^2) \right) \phi_{k3}(\boldsymbol{x}) \\ &+ \sum_{i=4}^{N} \alpha_{ke}^{(|a_i|)} \left(\partial^{a_i} c_h(\boldsymbol{x}_{kc}) (\Delta \boldsymbol{x}_k)^{a_i} \right) \phi_{ki}(\boldsymbol{x}). \end{aligned} \tag{31}$$

D. Slope limiting in time-dependent problems

For the given full-discrete scheme in Section 3, the slope limiter is applied to each discrete solution $C_m^{n,[k]}$ which can obtain a more stable modified numerical scheme. However, due to an implicit coupling between the spatial derivatives and the time derivatives is existing [22], we apply the slope limiter not only to the provisional solutions of each substep, but also to the time derivative $\dot{C} = \partial_t C$.

Let Φ^{Taylor} represent the slope limiting operator that applies any of the above slope limiting procedures to a global representation vector $C^{\text{Taylor}(t)}$ of a solution $c_h(t)$ in Taylor basis representation. The semi-discrete system (9) can be written in a Taylor basis,

$$M_c \partial_t C^{\text{Taylor}}(t) = S^{\text{Taylor}} \left(C^{\text{Taylor}}(t), t \right). \tag{32}$$

Then, the time derivative under Taylor basis is denoted as follows

$$\dot{C}^{\text{Taylor},(i)} := \partial_t C^{\text{Taylor}}(t_i) = M_c^{-1} \ S^{\text{Taylor}} \left(C^{\text{Taylor}}(t_i), t_i \right). \tag{33}$$

Under the action of the slope limiting operator, we have

$$\begin{aligned} M_L \partial_t C^{\text{Taylor}}(t) =& S^{\text{Taylor}} \left(\Phi^{\text{Taylor}} C^{\text{Taylor}}(t), t \right) \\ &+ (M_L - M_c) \Phi^{\text{Taylor}}(t) \partial_t C^{\text{Taylor}}(t), \end{aligned} \tag{34}$$

where $M_c = \{m_{ij}\}$, $M_L = \text{diag}\{m_{ii}\}$.

The modified derivative is defined by

$$\begin{aligned} \tilde{C}^{\text{Taylor},(i)} =& \partial_t C^{\text{Taylor}}(t_i) = M_L^{-1} \Big[S^{\text{Taylor}} \left(\Phi^{\text{Taylor}} C^{\text{Taylor}}(t_i), t_i \right) \\ &+ (M_L - M_c) \Phi^{\text{Taylor}}(t_i) \partial_t C^{\text{Taylor}}(t_i) \Big]. \end{aligned} \tag{35}$$

To eliminate the implicit coupling, we reformulate the modified time derivative in Taylor basis as

$$\begin{aligned} \tilde{C}^{\text{Taylor},(i)} =& \Phi^{\text{Taylor}} \dot{C}^{\text{Taylor},(i)} \\ &+ M_L^{-1} M_c \left(\dot{C}^{\text{Taylor},(i)} - \Phi^{\text{Taylor}} \dot{C}^{\text{Taylor},(i)} \right). \end{aligned} \tag{36}$$

Using (24) and (32), we rearrange the equation (36) to get the follow equation

$$\begin{aligned} \tilde{C}^{(i)} =& M^{-1} M^{\text{Taylor}} \Big[\Phi^{\text{Taylor}} \dot{C}^{\text{Taylor},(i)} \\ &+ M_L^{-1} M_c \left(\dot{C}^{\text{Taylor},(i)} - \Phi^{\text{Taylor}} \dot{C}^{\text{Taylor},(i)} \right) \Big], \end{aligned} \tag{37}$$

where $\dot{C}^{\text{Talor},(i)} := (M^{\text{Taylor}})^{-1} M \dot{C}^{(i)}$. Therefore, under the modification of slope limiters, we have $\partial_t C^{\text{Taylor}}(t) = \tilde{C}^{(i)}$. Then, the modified full-discrete scheme is given as follows

Predictor:

$$C_m^{n,[0]} = \Phi \Big[C_{m-1}^{n,[0]} + \tilde{H}_{m-1} \left(\tilde{C}^{[0]}(t_{m-1}^n) \right) \Big], \ m = 1, \cdots, M, \tag{38}$$

with $\tilde{H}_{m-1} \left(\tilde{C}^{[0]}(t_{m-1}^n) \right) = \Delta t_m^n \tilde{C}^{[0]}(t_{m-1}^n)$,

Corrector:

$$\begin{aligned} C_m^{n,[k+1]} =& \Phi \Big[C_{m-1}^{n,[k]} + \tilde{H}_{m-1} \left(\tilde{C}^{[k+1]}(t_{m-1}^n) \right) \\ &- \tilde{H}_{m-1} \left(\tilde{C}^{[k]}(t_{m-1}^n) \right) + \int_{t_{m-1}^n}^{t_m^n} I \tilde{C}^{[k]}(\tau) d\tau \Big], \end{aligned} \tag{39}$$

where the slope limiting operator Φ defined as

$$\Phi = M^{-1} M^{\text{Taylor}} \Phi^{Taylor} \left(M^{\text{Taylor}} \right)^{-1} M.$$

Similar to the formula (19), the last term in (39) is approximated by

$$\tilde{S}_n^k := \int_{t_{m-1}^n}^{t_m^n} I \tilde{C}^{[k]}(\tau) d\tau = \Delta t_m^n \sum_{m=0}^{M} w_{n,m}^s I \tilde{C}^{[k]}(t_m^n). \tag{40}$$

The convergence order of modified full-discrete scheme can up to $2M+1$ at the final time t_{End} of a single interval and $2M$ when repeated the stepping through a sequence of multiple interval, every sweep, ideally, elevates the order by one, until reaching the maximum order [24]. However, the stiff terms, boundary conditions and slope limiters may affect convergence such that more iterations are required the optimal order.

TABLE I: The orders of convergence in space for different polynomial degrees ($p = 1, 2$) and limiter types.

limiter	p / j	1 / $\|\|e_c\|\|$	1 / order	2 / $\|\|e_c\|\|$	2 / order
None	0	5.56e-2	-	9.26e-3	-
	1	1.46e-2	1.92	7.59e-4	3.61
	2	3.73e-3	1.97	7.99e-5	3.24
	3	9.34e-4	1.99	9.46e-6	3.07
	4	3.33e-4	2.01	1.16e-6	3.02
Linear	0	2.24e-1	-	2.21e-1	-
	1	5.04e-2	2.15	5.22e-2	2.08
	2	9.42e-3	2.42	1.03e-2	2.34
	3	1.46e-3	2.68	1.41e-3	2.87
	4	2.84e-4	2.36	2.13e-4	2.73
Hier.vert.based	0	2.24e-1	-	2.95e-1	-
	1	5.04e-2	2.15	2.65e-1	0.17
	2	9.42e-3	2.42	1.11e-1	1.25
	3	1.46e-3	2.68	7.71e-3	3.86
	4	2.84e-4	2.36	8.12e-4	3.25

V. Numerical experiments

A. Analytical convergence test

In order to prove that the proposed modified DG-SDC scheme can achieve higher-order accuracy in time and space, the analytical convergence tests will be carried out. For two-dimensional advection equation with variable coefficients, we choose the exact solution of the concentration

$$c(\boldsymbol{x}, t) = cos(7x^1)cos(7x^2) + e^{-t},\ \ t \in [0, 2\pi],\ \ \Omega = (0, 1)^2,$$

and velocity field

$$\boldsymbol{u}(\boldsymbol{x}, t) = [exp(x^1 + x^2)/2, exp(x^1 - x^2)/2].$$

The data c_D and f are derived analytically by inserting $c(\boldsymbol{x}, t)$ and $\boldsymbol{u}(\boldsymbol{x}, t)$ into (1). In this paper, the discrete error between the discrete solution $c_h(t)$ and the analytical solution $c(t)$ is calculated by $||e_c|| = ||c_h(t) - c(t)||_{L^2(\Omega)}$.

To calculate the order of spatial convergence, the element sizes are $h_j = \frac{1}{3\cdot 2^j}, j = 0, \cdots, 4$ and time step is $t = \frac{2\pi}{3000}$. The specific numerical results are shown in Table 1, where p is the polynomial of degree. It's worth noting that the Hierarchical vertex-based limiter is equivalent to linear limiter when the model basis is linear polynomial ($p = 1$). In addition, when the model basis is quadratic polynomial (p = 2), the proposed scheme achieve higher-order accuracy in spatial, and produce overconvergence under the action of the Hierarchical vertex-based limiter.

To calculate the order of time convergence, we select appropriate element size and carry out analytical convergence test for different time steps. In this paper, the element size is $h = \frac{1}{16}$ and the time steps are $\tau_j = 200+40\times 2^j,\ j = 1, \cdots, 5$. The convergence order of the different the number of subintervals M and corrections sweeps K are shown in Table 2. For simplicity, the number of subintervals is equal to the corrections sweeps, i.e., M = K = 2, 3, 4. In Table 2, with the increase of the number of subintervals and corrections sweeps of SDC method, the order of time convergence increases accordingly. When M = K = 1, the SDC discrete scheme is equivalent to the Euler discrete scheme. When M = K = 3, the order of time convergence of the proposed scheme up to order 3. Further, when M = K = 4, the order of time convergence of the proposed scheme up to order 6.

TABLE II: The orders of convergence in time for different the number of subintervals M and corrections sweeps K.

M(= K) / j	2 / $\|\|e_c\|\|$	2 / order	3 / $\|\|e_c\|\|$	3 / order	4 / $\|\|e_c\|\|$	4 / order
1	1.03e-2	-	4.45e-1	-	9.54e-1	-
2	6.89e-3	1.61	1.49e-1	4.32	3.97e-1	6.32
3	3.65e-3	1.72	3.96e-2	3.62	8.73e-2	6.03
4	1.32e-3	2.11	6.81e-3	3.67	1.44e-2	4.91
5	6.72e-4	1.21	1,12e-3	3.19	1.30e-3	5.01

B. Solid body rotation

To test the performance of two kinds of slope limiters, we use solid body rotation test proposed by LeVeque [15], which is a classical numerical example to investigate limiters performance. It consists of a slotted cylinder, a sharp cone, and a smooth hump that are placed in a square domain $\Omega = [0, 1]^2$ and transported by a time-independent velocity field $\boldsymbol{u}(\boldsymbol{x}) = [0.5-x^2, x^1-0.5]^T$ in a counterclockwise rotation over $J = (0, 2\pi)$. With $r = 0.0225$ and $G(\boldsymbol{x}, \boldsymbol{x}_0) = \frac{1}{0.15}||\boldsymbol{x} - \boldsymbol{x_0}||_2$, we choose the initial data satisfying

$$c^0(\boldsymbol{x}) = \begin{cases} 1,\ \text{if} & \begin{array}{l}(x^1-0.5)^2 + (x^2-0.75)^2 \geq r \\ \wedge\, (x^1 \leq 0.475 \vee x^1 \geq 0.525 \vee x^2 \geq 0.85)\end{array} \\ 1 - G(\boldsymbol{x}, [0.5, 0.25]^T),\ \text{if} & \begin{array}{l}(x^1-0.5)^2 \\ + (x^2-0.25)^2 \leq r\end{array} \\ \frac{1}{4}\left(1 + cos\left(\pi\ G(\boldsymbol{x}, [0.25, 0.5]^T)\right)\right),\ \text{if} & \begin{array}{l}(x^1-0.25)^2 \\ + (x^2-0.5)^2 \\ \leq r\end{array} \\ 0,\ \text{otherwise} & \end{cases}$$

The $c_D = 0$ and $f = 0$ are boundary data and right-hand side term, respectively. The specific numerical results are shown in Figure 1-4. The numerical scheme produces very obvious spurious oscillation in Figure 2. But the linear and the hierarchical limiters appear well perform in Figure 3 and Figure 4, it is proved that the two kinds of limiters can effectively control the spurious oscillation. In addition, the hierarchical vertex-based limiter could maintain the higher-order accuracy and effectively control the numerical oscillation.

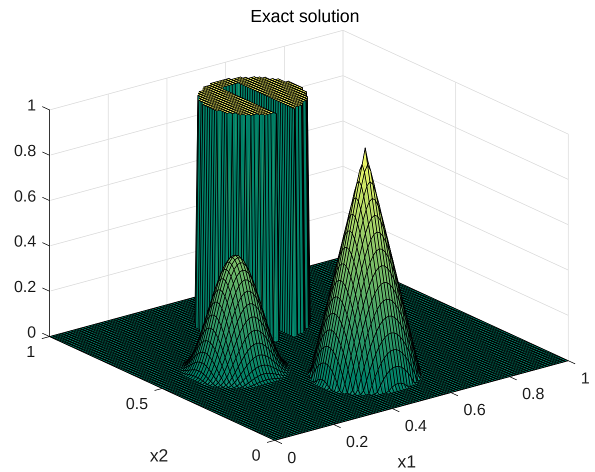

Fig. 1: Exact solution.

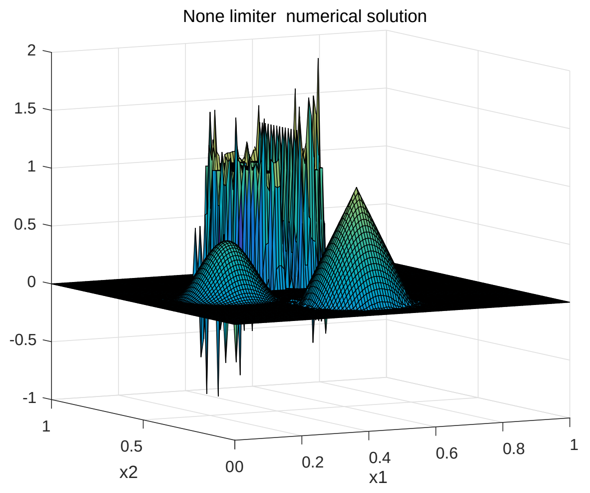

Fig. 2: Numerical solution of DG-SDC scheme.

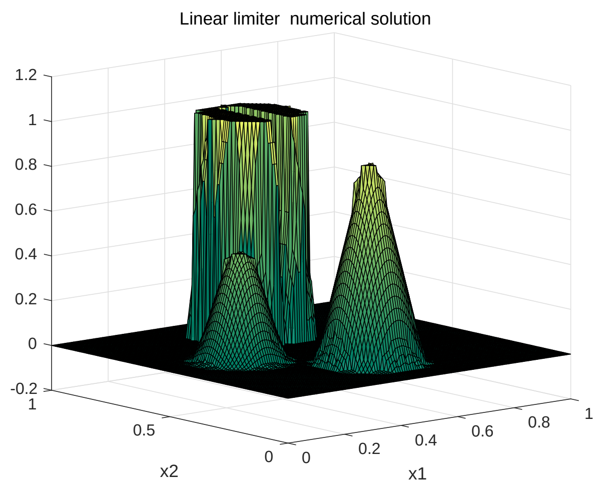

Fig. 3: Numerical solution of DG-SDC scheme modified by linear limiter.

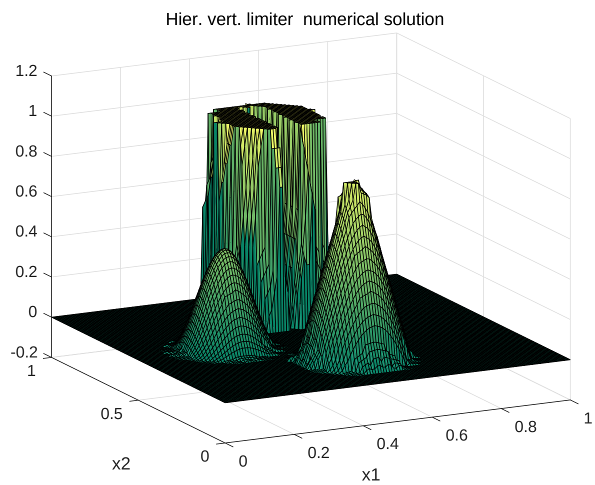

Fig. 4: Numerical solution of DG-SDC scheme modified by Hier. vert. limiter.

VI. Conclusion

In this paper, a numerical scheme based on DG-SDC method is proposed for the advection equation with variable coefficients. In addition, in order to prevent the onset of spurious oscillations, two kinds of slope limiters are applied to correct this novel numerical scheme. This novel numerical scheme can achieve arbitrary higher-order convergence in space and time simultaneously. Furthermore, the higher-order accuracy, efficiency and stability of the presented scheme are demonstrated through numerical examples. Next, we consider applying the presented scheme to solve more complex models.

References

[1] G. Andrew, K. Lilia, Analysis of slope limiters on unstructured triangular meshes, J. Comput. Phys., vol. 374, no. 1, pp. 1-26, 2018.

[2] D. N. Arnold, F. Brezzi, B. Cockburn, L. D. Marini, Unifited analysis of discontinous Calerkin methods for elliptic problems, SIAM J. Numer. Anal., vol. 39, no. 5, pp. 1749-1779, 2002.

[3] T. Buvoli, A class of exponential integrators based on spectral defferred correction, SIAM J. Sci. Comput., vol. 42, no.1, pp. 1-27, 2020.

[4] M. D. Bragin, Y. AKriksin, V. F. Tishkin, A discontinuous Galerkin method with an entropic slope limiter for Euler equations, Math. Models Comput. Simul., vol. 24, no. 12, pp. 824-833, 2020.

[5] E. M. Constantinescu, A. Sandu, Extrapolated implict-explicit time stepping, SIAM. J. Sci. Comput., vol. 31, no. 6, pp. 4452-4477, 2010.

[6] A. Dutt, L. Greengard, V. Rokhlin, Spectral deferred correction methods for ordinary differential equations, BIT Numer. Math., vol. 40, no. 2, pp. 241-266, 2000.

[7] K. Dutt, L. Krivodonova, A high-order moment limiter for the discontinuous Galerkin method on triangular meshes, J. Comput. Phys., vol. 433, no. 15, pp. 110-188, 2021.

[8] F. Frank, B. Reuter, V. Aizinger, P. Knaber, FESTUNG: A MATLAB/GUN Octave toolbox for the discontinuous Galerkin method, Part I: Diffusion Operator, Comput. Math. Appl., vol. 70, no. 1, pp. 11-46, 2015.

[9] Y. Gu, Q. S. Hua, C. Z. Zhang, X. Q. He, The generalized finite difference method for long-time transient heat conduction in 3D anisotropic composite materials, Appl. Math. Model., Vol. 71, pp. 316-330, 2019.

[10] P. H. Francois, M. Schreiber, L. M. Michael, Multi-level spectral deferred corrections scheme for the shallow water equations on the rotating sphere, J. Comput. Phys., vol. 376, no. 1, pp. 435-454, 2019.

[11] H. Hennes, D. Kuzmin, V. Aizinger, New directional vector limiters for discontinuous Galerkin methods, J. Comput. Phys., vol. 384, pp. 308-325, 2019.

[12] D. Kuzmin, A vertex-based hierarchical slope limiter for p-adaptive discontinuous Galerkin methods, J. Comput. Appl. Math., vol. 233, no. 12, pp. 3077-3085, 2010.

[13] D. Kuzmin, Slope limiting for discontinuos Glarkin approximations with a possibly non-orthogonal Taylor basis, Internat. J. Numer. Methods Fluids., vol. 71, no. 9, pp. 1178-1190, 2013.

[14] W. Kress, B. Gustafsson, Defferred correction methods for initial boundary value problems, J. Sci. Comput., vol. 17, no. 1/4, pp. 241-251, 2002.

[15] R. J. Leveque, High-resolution conservative algorithms for advection in incompressible flow, SIAM J. Numer. Anal., vol. 33, no. 2, pp. 627-665, 1996.

[16] Y. Liu, C. W. Shu, M. P. Zhang, Sub-optimal convergence of discontinuous Galerkin methods with central fluxes for linear hyperbolic equations with even degree polynomial approximations, J. Comput. Math., vol. 39, no. 4, pp. 518-537, 2021.

[17] A. Naveed, M. Gunar, Higher-order discontinuous Galerkin time discretizations for the evolutionary Navier-Stokes equations, IMA J. Numer. Anal., vol. 41, no. 4, pp. 3113-3144, 2021.

[18] L. Qian, H. Cai, Implicit-Explicit Time Stepping Scheme Based on the Streamline Diffusion Method for Fluid-fluid Interaction Problems, IAENG International Journal of Applied Mathematics, vol. 48, no. 3, pp. 278-287, 2018.

[19] F. Qing, X. J. Yu, Z. P. Jia, Z. Z. Li, A cell-centered Lagrangian discontinuous Galerkin method using WENO and HWENO limiter for compressible Euler equations in two dimensions, Comput. Appl. Math., vol. 211, no. 40, pp. 233-266, 2021.

[20] M. M. Rahman, Compromising with corrector step of SIMPLE algorithm, Math. Comput. Simul. vol. 188, pp. 135-163, 2021.

[21] H. Reed, T. R. Hill, Triangular Mesh Methods for The Neutron Transport Equation, Tech. Rep. LA-UR-73-479. Los alamos report La., 1973.

[22] B. Reuter, V. Aizinger, M. Wieland, F. Frank, P. Knabner, FESTUNG: A MATLAB/GUN Octave toolbox for the discontinuous Galerkin method, part II: Advection operator and slope limiting, Comput. Math. Appl., vol. 72, no. 7, pp. 1896-1925, 2016..

[23] V. Stefan, B. Nicole, B. Jörn, A limiter-based well-balanced discontinuous Galerkin method for shallow-water flows with wetting and drying: triangular grids, Internat. J. Numer. Methods Fluids., vol. 91, no. 8, pp. 395-418, 2019.

[24] J. Stiller, A spectral deffered correction method for incompressible flow with variable viscosity, J. Comput. Phys., vol. 423, 109840, 2020.

[25] Q. H. Tran, Second-order slope limiters for the simultaneous linear advection of (not so) independent variables, Commun. Math. Sci., vol. 6, no. 3, pp. 569-593, 2008.

[26] L. Wang, P.-O. persson, A high-order discontinuous Galerkin method with unstructure spacetime meshs for two-dimensional compressible flows on domains with large deformations, Comput. Fluids., vol. 118, pp. 53-68, 2015.

[27] Z. F. Weng, Y. P. Zeng, S. Y. Zhai, The operator splitting method with semi-implicit spectral deferred correction for molecular beam epitaxial growth models, J. Algorithms Comput. Technol., vol. 14, 2020.

[28] J. Zhu, J. Qiu, C. W. Shu, High-order Runge-Kutta discontinuous Galerkin methods with a new type of mulyi-resolution WENO limiters, J. Comput. phys., vol. 404, no. 4, 109105, 2020.

[29] J. Zhu, C. W. Shu, J. X. Qiu, High-order Runge-Kutta discontinuous Galerkin methods with multi-resolution WENO limiters for solving steady-state problems, Appl. Numer. Math., vol. 165, pp. 482-499, 2021.

Jing Wang was born in Shaoyang, Hunan Province, china, in 1998. The author is a graduate student in computational mathematics at Guangxi Normal University, Guilin, Guangxi Zhuang Autonomous Region, China, starting in 2020.

The author current research interests include numerical solution of partial differential equations and computing sciences, fluids and fluid-fluid interaction problems, discontinuous Galerkin finite element method.

Chun-ya Wu was born in Hezhou, Guangxi Zhuang Autonomous Region, china, in 1998. The author is a graduate student in computational mathematics at Guangxi Normal University, Guilin, Guangxi Zhuang Autonomous Region, China, starting in 2020.

The author current research interests include numerical solution of partial differential equations and computing sciences, fluids and fluid-fluid interaction problems, two-phase fluids.

Ling-zhi Qian was born in Lingbi, Anhui Province, china, in 1980. The author received his Ph. D. in computational mathematics at Nanjing Normal University, Nanjing, Jiangsu Province, China, in June 2016.

The author current research interests include numerical solution of partial differential equations and computing sciences, fluids and fluid-fluid interaction problems, two-phase fluids.